

The Spatiotemporal Variability of Cloud Radiative Effects on the Greenland Ice Sheet Surface Mass Balance

Izeboud, M.; Lhermitte, S.; Van Tricht, K.; Lenaerts, J. T.M.; Van Lipzig, N. P.M.; Wever, N.

DOI

[10.1029/2020GL087315](https://doi.org/10.1029/2020GL087315)

Publication date

2020

Document Version

Final published version

Published in

Geophysical Research Letters

Citation (APA)

Izeboud, M., Lhermitte, S., Van Tricht, K., Lenaerts, J. T. M., Van Lipzig, N. P. M., & Wever, N. (2020). The Spatiotemporal Variability of Cloud Radiative Effects on the Greenland Ice Sheet Surface Mass Balance. *Geophysical Research Letters*, 47(12), Article e2020GL087315. <https://doi.org/10.1029/2020GL087315>

Important note

To cite this publication, please use the final published version (if applicable). Please check the document version above.

Copyright

Other than for strictly personal use, it is not permitted to download, forward or distribute the text or part of it, without the consent of the author(s) and/or copyright holder(s), unless the work is under an open content license such as Creative Commons.

Takedown policy

Please contact us and provide details if you believe this document breaches copyrights. We will remove access to the work immediately and investigate your claim.



RESEARCH LETTER

10.1029/2020GL087315

The Spatiotemporal Variability of Cloud Radiative Effects on the Greenland Ice Sheet Surface Mass Balance

M. Izeboud¹, S. Lhermitte¹, K. Van Tricht², J. T. M. Lenaerts³, N. P. M. Van Lipzig⁴, and N. Wever³

¹Department of Geoscience and Remote Sensing, Delft University of Technology, Delft, The Netherlands, ²VITO Remote Sensing, Mol, Belgium, ³Department of Atmospheric and Oceanic Sciences, University of Colorado Boulder, Boulder, CO, USA, ⁴KU Leuven, Leuven, Belgium

Key Points:

- Total cloud radiative warming occurs year-round, except in the ablation area during summer
- When cloud radiative cooling occurs, clouds reduce mass loss and dominate the impact on the surface
- Short-term and long-term cloud effects are opposite, governed by surface albedo changes

Supporting Information:

- Supporting Information S1
- Figure S1
- Figure S2
- Figure S3
- Figure S4
- Figure S5
- Figure S6
- Figure S7

Correspondence to:

M. Izeboud,
m.izeboud@tudelft.nl

Citation:

Izeboud, M., Lhermitte, S., Van Tricht, K., Lenaerts, J. T. M., Van Lipzig, N. P. M., & Wever, N. (2020). The spatiotemporal variability of cloud radiative effects on the Greenland ice sheet surface mass balance. *Geophysical Research Letters*, 47, e2020GL087315. <https://doi.org/10.1029/2020GL087315>

Received 11 FEB 2020

Accepted 21 MAY 2020

Accepted article online 4 JUN 2020

Abstract To better understand and quantify the impact of clouds on the Greenland Ice Sheet surface mass balance (SMB), we study the spatiotemporal variability of the cloud radiative effect (CRE). The total CRE is separated in short-term and long-term impacts by performing multiple simulations with the SNOWPACK model for 2001–2010. The annual total CRE is $16.8 \pm 4.5 \text{ W m}^{-2}$, reducing the SMB with $-157 \pm 3.8 \text{ Gt yr}^{-1}$. Summer cloud radiative cooling is $-6.4 \pm 5.7 \text{ W m}^{-2}$ in the ablation area, increasing the SMB with $121 \pm 2.2 \text{ Gt yr}^{-1}$. The annual integrated impact is cloud-reduced SMB of -36 Gt yr^{-1} . The short-term effect dominates the opposing long-term effects through the albedo-melt feedback. A long-term warming effect decreases the albedo and so preconditions the surface for enhanced (summer) melt. The impact of the CRE, determined by spatial, temporal and initial conditions, explains existing conflicted views on the role of cloud radiation and emphasizes the need for accurate cloud and albedo representations in future studies.

1. Introduction

The Greenland ice sheet (GrIS) has been losing mass since the late 1990s primarily through a rise in surface meltwater runoff (Fettweis, Franco, et al., 2013; van den Broeke et al., 2016). The rise in meltwater runoff is mainly attributed to more frequent warm and dry summers (Fettweis, Hanna, et al., 2013) and a decrease in surface albedo (Box et al., 2012). Clouds regulate the amount of radiation received by the surface, which determines surface melt, and can trigger feedback mechanisms that induce albedo changes (Bintanja & Van Den Broeke, 1996). This is the cloud radiative effect (CRE). Clouds block shortwave (SW) radiation which limits the albedo melt feedback, reducing melt. Moreover, clouds directly increase the broadband surface albedo by shifting direct solar radiation to diffuse radiation (Gardner & Sharp, 2010). Yet clouds enhance the amount of longwave (LW) radiation by reemitting the heat lost from the surface, enhancing melt. Over polar regions, the increase in LW radiation (warming effect) generally dominates the decrease in SW radiation (cooling effect) during winter and vice versa for summer (Curry et al., 1996). A warming CRE affects the conditions of the GrIS surface snow/firn, reducing meltwater refreezing and thereby accelerating bare-ice exposure (decreasing the albedo) and enhancing meltwater runoff, as discussed by Van Tricht et al. (2016). However, Hofer et al. (2017) argue that the observed decreasing summer cloud cover, a relative increase in SW radiation, is the main driver for the increase in meltwater runoff. Furthermore, Wang et al. (2018) argue that clouds limit the albedo feedback and decelerate surface melt, referring to a net cooling CRE observed by automatic weather stations. Recently, the deceleration of accelerated GrIS melting since 2013 is linked by Ruan et al. (2019) to the reduction in SW radiation in the presence of increasing total cloud cover.

These studies show conflicting views on the role of cloud effects on the LW and SW radiation, and the impact on the GrIS surface mass balance (SMB): Do clouds limit the albedo melt feedback and reduce melt, or is the warming effect of clouds crucial for the amount of surface melt? Where Hofer et al. (2017) conclude the first, while focused mainly on the ablation area, Van Tricht et al. (2016) conclude the second for the complete GrIS and Wang et al. (2019) show a spatial contrast between the ablation and accumulation area. Moreover, the studies do not all cover the seasonal variations.

In this study we aim to combine all temporal and spatial variations of the CRE and quantify their impact, in order to resolve existing discrepancies. In order to link the CRE to the SMB, we apply different atmospheric forcing scenarios (obtained from the regional climate model RACMO2.3p2, Van Wessem et al., 2018) to

©2020. The Authors.

This is an open access article under the terms of the Creative Commons Attribution License, which permits use, distribution and reproduction in any medium, provided the original work is properly cited.

the snow model SNOWPACK (Lehning et al., 2002). The simulations are done to determine the seasonal variations of (total) CRE and separate this into a short-term and long-term components. The short-term effect is determined as a (sub)daily CRE while the long-term effect represents lasting changes to surface conditions. The offline configuration of SNOWPACK enables the possibility to quantify the impact of purely the CRE and its separate temporal components, while keeping other parameters constant.

2. Methods and Data

The CRE (W m^{-2}) is defined as the difference in net radiation fluxes (F_{SW}^{\uparrow} and F_{LW}^{\uparrow} for net shortwave and long-wave radiation, respectively) of an all-sky scenario to a clear-sky scenario simulation, defined in Equation 1:

$$\text{CRE} = \left(F_{\text{SW,all-sky}}^{\uparrow} + F_{\text{LW,all-sky}}^{\uparrow} \right) - \left(F_{\text{SW,clear-sky}}^{\uparrow} + F_{\text{LW,clear-sky}}^{\uparrow} \right) \quad (1)$$

The all-sky scenario provides the GrIS meteorology as given by the regional climate model RACMO2.3p2 (Van Wessem et al., 2018). In the clear-sky scenario, all clouds and their radiative effects are removed. Precipitation (solid and liquid), temperature, wind speed, and relative humidity are not adapted to exclude their impacts on the surface conditions. A positive CRE indicates net cloud warming at the surface; a negative CRE indicates net cloud cooling.

The impact of the cloud radiative forcing on the SMB can be determined similarly as the CRE, by comparing the respective all-sky to clear-sky scenarios ($\text{SMB}_{\text{all-sky}} - \text{SMB}_{\text{clear-sky}}$). The cloud impact on the SMB is therefore always in a relative sense and is described as “cloud-enhanced” SMB or “cloud-reduced” SMB. A cloud-reduced SMB represents a relative mass loss, a decrease in SMB: A negative SMB (ablation) will be more negative due to clouds, or a positive SMB (accumulation) will be less positive. Similarly, for cloud-enhanced SMB, which represents a relative mass increase.

The methodology used in this study builds upon the methodology of Van Tricht et al. (2016): The snow model SNOWPACK is forced with atmospheric conditions of either the all-sky or clear-sky scenario, to assess the impact of the CRE on the SMB. Our approach differs from the original Van Tricht et al. (2016) method in three distinct ways. We do not use their hybrid data set (a combination of RACMO2.3 and CloudSat-CALIPSO radiative flux data) but instead only use the RACMO2.3p2 model data. This is justified by the improved version of RACMO2.3p2 compared to RACMO2.3 (Van Wessem et al., 2018) and by the added benefits this brings: First, the studied period is extended to 2001–2010 instead of 2007–2010 which better accounts for interannual variability. Second, the simulations are performed on the RACMO2.3p2 model grid resolution of 5.5 km^2 instead of $2 \times 2^\circ$ grid boxes, such that the ablation area and accumulation area can be clearly distinguished. Third, the simulation scenarios are expanded, to cover both short-term and long-term effects, as described in section 2.2.

2.1. SNOWPACK Simulations

SNOWPACK is a one-dimensional (depth) physics-based snow and land-surface model that contains a detailed description of the mass and energy exchange between the snow and the atmosphere (Lehning et al., 2002). SNOWPACK gives as output a set of time series that describe the snow profile and its processes. To better represent GrIS snow conditions, SNOWPACK has been refined to include a prognostic snow albedo parameterization (Gardner & Sharp, 2010; van Angelen, 2012) that accounts for snow grain size variations, cloud optical depth, solar zenith angle, and concentration of light-absorbing impurities at the surface. Supporting information Figure S1 shows a good correlation between SNOWPACK GrIS and RACMO2.3p2 SMB, with a bias of $0.02 \text{ m w.e. yr}^{-1}$ and RMSE of $0.6 \text{ m w.e. yr}^{-1}$ over a 10-yr period. Though it should be noted that the overestimation of the SMB by SNOWPACK, that is, an underestimation of the ablation rate, means that cloud effects on the ablation rate will be underestimated. The mean bias for the ablation rate ($\text{SMB} < 0$) is $0.03 \text{ m w.e. yr}^{-1}$.

To couple the effect of clouds on the surface energy balance (SEB) to the SMB, SNOWPACK simulations were performed for the all-sky and clear-sky scenario. The snow model provides output for both SEB and SMB components, thus enabling the quantification of the CRE and its impact on the GrIS surface. To save computational resources simulations were performed at three different spatial resolutions: 5.5 km^2 for the ablation area, the bulk of the accumulation area at 22 km^2 and the rest (determined as the area where the RACMO surface albedo does not drop below 0.7) at 44 km^2 .

Output time series are given for each simulated grid point. Spatial averaged values provided in this paper, for either ablation area, accumulation area, or GrIS wide, are weighted for each individual grid point (i) area (A_i),

$$\bar{x} = \frac{\sum_{i=1}^N x_i A_i}{\sum_{i=1}^N A_i}, \quad (2)$$

where N is the number of grid points in the respective area. For the CRE, x is calculated as a seasonal or annual average. For mass balance terms, x is calculated as a seasonal or annual integrated value.

2.2. Scenarios

To gain insight in the temporal variability of the CRE, each day in 2001–2010 is simulated separately for the all-sky and clear-sky scheme. To distinguish between short-term (daily forcing) effects and long-term (continuous) effects, we also initialize the snow profile each day for both schemes. This is a fundamental difference to Van Tricht et al. (2016), who initialized only at the start of the simulation (2007) and subsequently only quantified the total CRE. Here, each day is initialized with preceding either only all-sky conditions or only clear-sky conditions. For both the all-sky initialization scheme (ASI) and clear-sky initialization scheme (CSI), each day is simulated twice: once for an all-sky day (AS) and once for a clear-sky (CS) day. The computational time step is 15 min, with output provided every 3 hr. As a result, we have four different scenarios:

1. ASI-AS: one all-sky day simulated, initialized with preceding all-sky conditions. This is the scenario corresponding to the “actual” model input, including all clouds and cloud effects.
2. ASI-CS: one clear-sky day simulated, initialized with preceding all-sky conditions.
3. CSI-AS: one all-sky day simulated, initialized with preceding clear-sky conditions.
4. CSI-CS: one clear-sky day simulated, initialized with preceding clear-sky conditions, that is, a scenario without clouds.

These four scenarios allow to separate the total CRE into short- and long-term cloud effects, where the following comparisons can be made:

1. Total CRE: difference between scenario ASI-AS to CSI-CS (1–4), that is, all clouds compared to always clear-sky conditions.
2. Short-term CRE: difference between scenario ASI-AS to ASI-CS (1–2) and scenario CSI-AS to CSI-CS (3–4). These schemes have the same initial snow/firn conditions, but different cloud forcing for each day. From here on, short-term effect referred to represents the average of both (1–2) and (3–4).
3. Long-term CRE: difference between scenario ASI-AS to CSI-AS (1–3) and scenario ASI-CS to CSI-CS (2–4). These schemes show the difference between the conditions of the snow/firn layers due to the initialization approach. From here on, long-term effect referred to represents the average of both (1–3) and (2–4).

Both components of the short-term (and respectively long-term) effect yield very similar results: The mean bias between the two short-term components is 0.1 W m^{-2} , for the two long-term components is 0.2 W m^{-2} . This is why both components are averaged to give one short-term result and one long-term result.

3. Results

3.1. Seasonal Variations of Cloud Radiative Effect

Figure 1 shows that the CRE as calculated by our simulations exhibits a clear spatial and temporal variability. For winter (December, January, February, DJF), spring (March, April, May, MAM), and fall (September, October, November, SON), the CRE is positive on the entirety of the GrIS, inducing a net warming effect at the surface. The total CRE is, respectively, $20.4 \pm 4.7 \text{ W m}^{-2}$ (SON), $18.2 \pm 4.3 \text{ W m}^{-2}$ (DJF), $14.7 \pm 4.4 \text{ W m}^{-2}$ (MAM), and $13.8 \pm 4.5 \text{ W m}^{-2}$ (June, July, August, JJA), over the period 2001–2011 (see Figure 1a). However, during summer, a negative total CRE is found in the ablation area, forming a stark contrast to the accumulation area, where the CRE is positive year-round. The clear spatial contrast between summer cloud radiative warming and cooling was not found by Van Tricht et al. (2016), and can be attributed to the current

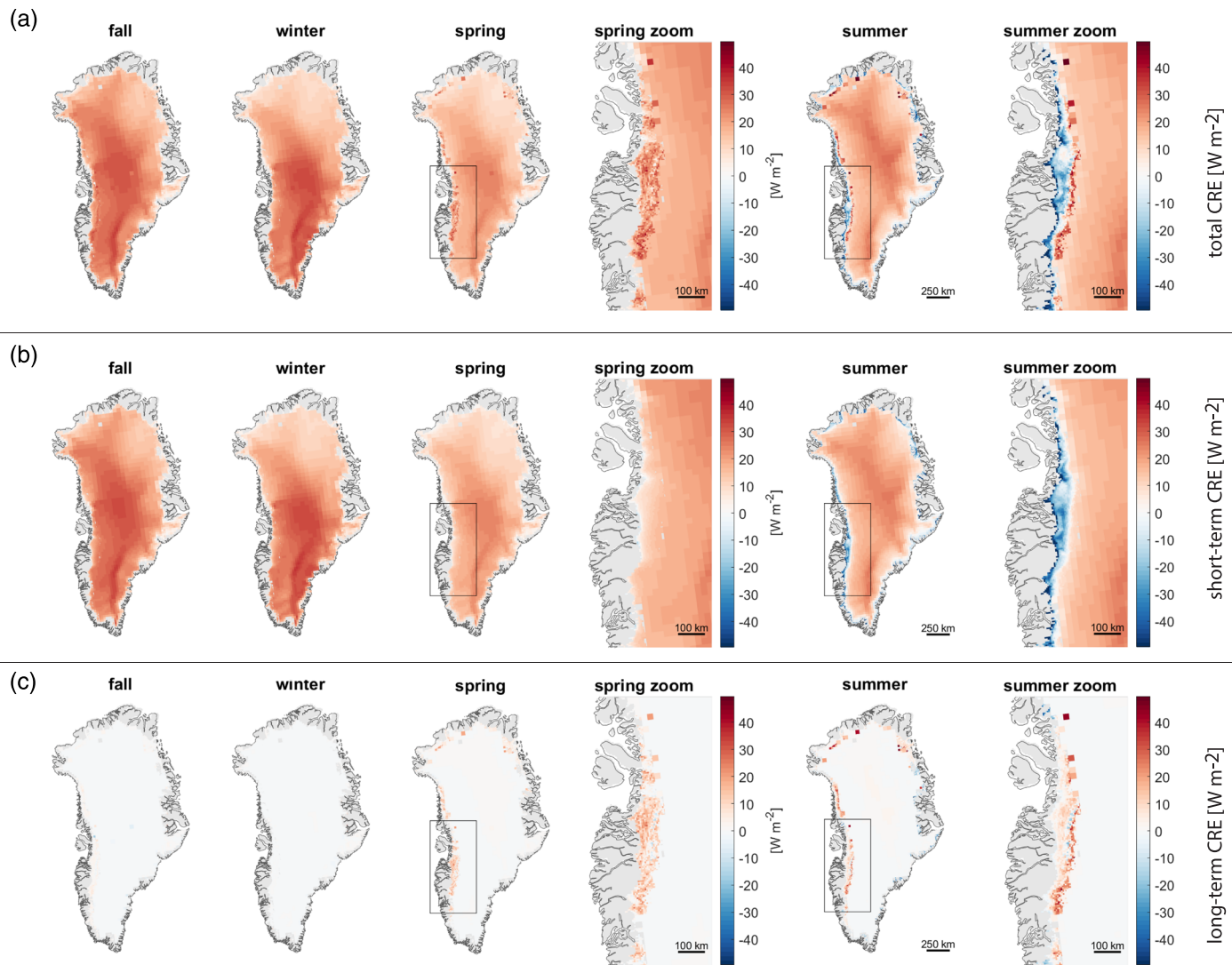


Figure 1. Cloud radiative effect (CRE, W m^{-2}) on the GrIS (2001–2010), averaged per season for (a) total CRE, (b) short-term CRE (daily), and (c) long-term CRE (continuous).

higher resolution of the simulations. The total cooling effect in the ablation area in summer is on average $-6.4 \pm 5.7 \text{ W m}^{-2}$, in contrast to the warming effects more inland of $15.7 \pm 3.0 \text{ W m}^{-2}$, covering a much larger area (approximate ratio of 1 to 10) and therefore resulting in the GrIS wide summer cloud radiative warming effect. The spatial variability of the net CRE shown here are similar to results of Wang et al. (2019): a small band of summer cloud radiative cooling at the coast, and cloud radiative warming inland of the GrIS.

As shown in Figures 1b and 1c, our results demonstrate a large difference between the contribution of the short-term and long-term effects to the total CRE, both spatially and temporally. See also supporting information Figure S2 for the time series of both the ablation and accumulation area. The short-term effect is contrary to and dominates the long-term effect: When summer short-term cloud radiative cooling/warming occurs, long-term cloud radiative warming/cooling occurs. In the ablation area, the long-term CRE is of similar strength as the short-term warming effect during spring: respectively $5.8 \pm 11.2 \text{ W m}^{-2}$ and $6.8 \pm 3.1 \text{ W m}^{-2}$. For summer in the ablation area, the long-term warming CRE of $8.4 \pm 15.6 \text{ W m}^{-2}$ is as strong contrast to the short-term cooling CRE of $-6.4 \pm 5.7 \text{ W m}^{-2}$. The positive long-term CRE indicates a buffering of the radiative warming effects in the GrIS surface conditions. This buffering effect of atmospheric conditions on the GrIS surface is especially relevant during spring, when the stage for summer melt is set. Contrarily, the long-term effect at the accumulation area is a cooling effect (Figure 1c) and strongest

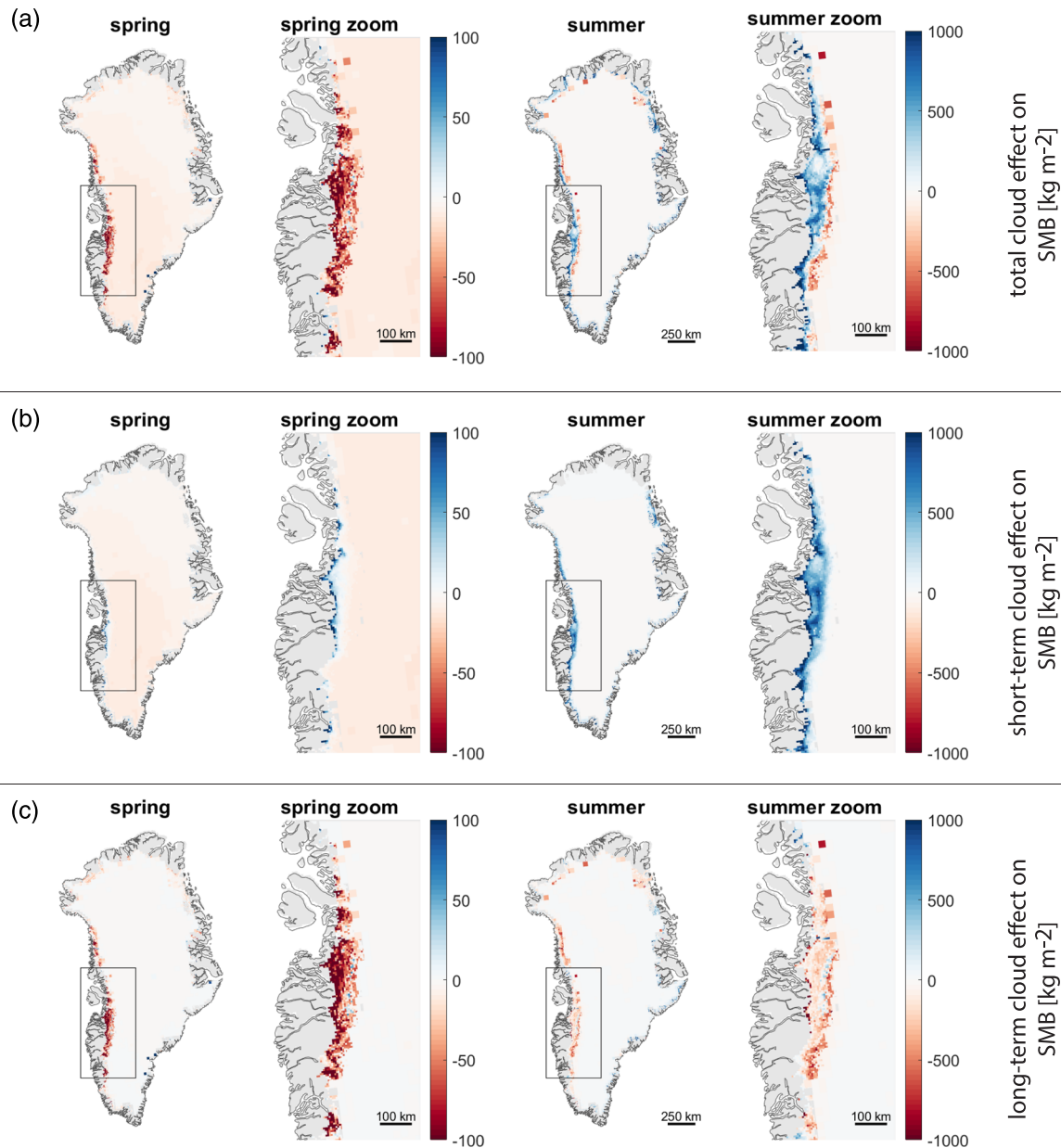


Figure 2. The impact of the CRE on the SMB in spring and summer, seasonal total (kg m^{-2}). (a) Total, (b) short-term, and (c) long-term cloud effect. Positive values (blue) indicate cloud-enhanced SMB (relative mass increase), negative values (red) indicate cloud-reduced SMB (relative mass loss). Note the change in scale used to visualize the seasons.

in summer, though it is only $-0.2 \pm 0.8 \text{ W m}^{-2}$ —insignificant compared to its accompanying summer short-term warming effect of $15.7 \pm 3.0 \text{ W m}^{-2}$.

3.2. Impact on SMB

The impact of the cloud radiative forcing on the SMB can be determined similarly as the CRE, by comparing the respective all-sky to clear-sky scenarios. The cloud impact on mass is therefore always in a relative sense. For mass terms, instead of computing the seasonal average, seasonal values are integrated per simulated grid point to result in a seasonal total mass contribution (kg m^{-2}). The impact of the CRE on the SMB is described as “cloud-enhanced” SMB (i.e., relative mass increase due to clouds) or “cloud-reduced” SMB (i.e., relative mass loss due to clouds). The impact on the SMB is, as expected, strongly and inversely correlated to the magnitude of the CRE: Cloud radiative warming corresponds to cloud-reduced SMB and cloud radiative cooling corresponds to cloud-enhanced SMB.

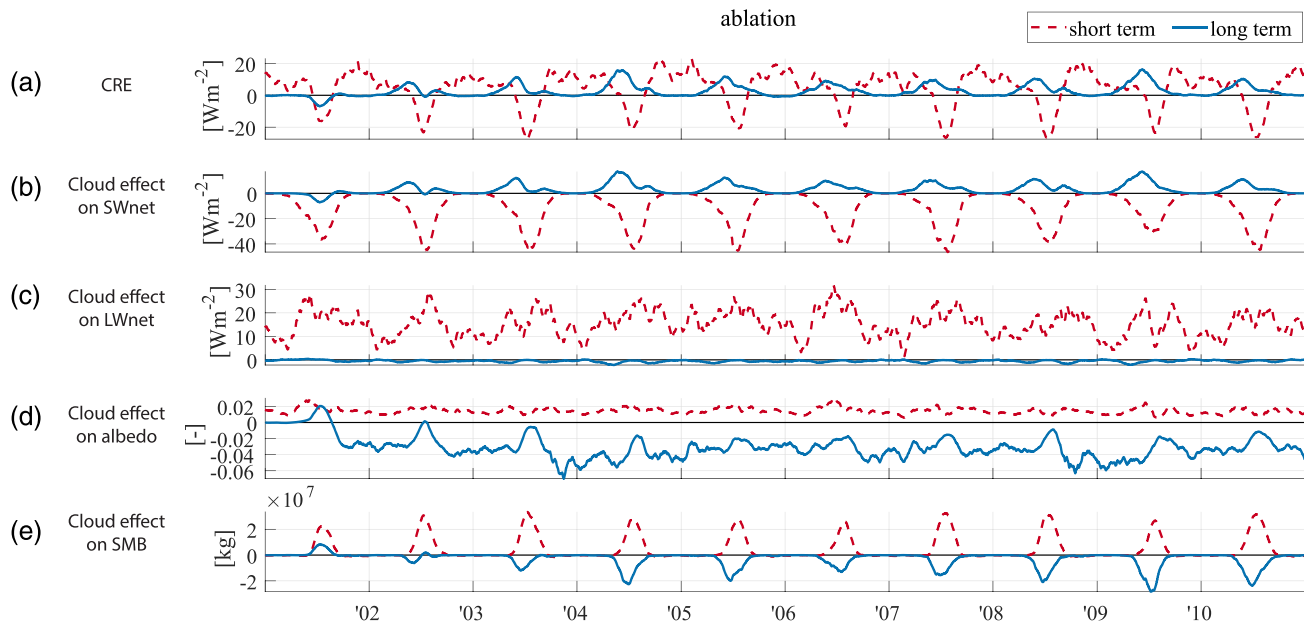


Figure 3. Time series for (a) net CRE, the CRE for (b) only SW radiation, (c) only LW radiation and the impact of the CRE on (d) the albedo and (e) the SMB. For each figure, a positive value indicates cloud-enhanced values (i.e., cloud-enhanced SMB means a relative increase in mass due to clouds). Plotted with a 30-day moving average.

Figure 2 shows the impact of the cloud radiative forcing on the SMB in spring and summer (supporting information Figure S3 includes fall and winter), for (a) the total cloud effect, (b) short-term and (c) long-term time scale. During the fall and winter seasons, the impact of the CRE on the SMB is dominated by sublimation effects. During the melt season, the CRE also impacts melt and refreezing rates. As can be expected, the effects are strongest in summer, and strongest in the ablation area through impact on melt.

On short-term time scale, cloud radiative warming in the accumulation area induces surface warming and enhances mass loss (cloud-reduced SMB); see Figure 2b. On one hand, this enhances surface snow sublimation, which occurs throughout the year (supporting information Figure S4). On the other hand, the reduction of LW heat loss (supporting information Figure S5c) reduces the amount of (nighttime) meltwater refreezing, thereby enhancing meltwater runoff. Both effects contribute to short-term cloud-reduced SMB in the accumulation area of $-1.1 \pm 0.3 \text{ kg m}^{-2}$ (MAM) and $-1.5 \pm 0.7 \text{ kg m}^{-2}$ (JJA). Contrarily, summer short-term cooling CRE in the ablation area directly reduces surface mass loss by reducing melt rates: cloud SW blocking reduces the amount of energy available for melt and limits the albedo melt feedback (Figure 3d). This results in short-term summer cloud-enhanced SMB of $37.3 \pm 12.2 \text{ kg m}^{-2}$: a much stronger impact per unit area than the cloud radiative warming impact.

The long-term impact of the CRE on the SMB, Figure 2c, is cloud-reduced SMB, corresponding to the prevailing long-term cloud warming effects in the ablation area. The cloud-reduced SMB (relative mass loss) is $-3.0 \pm 6.7 \text{ kg m}^{-2}$ (MAM) and $-16.1 \pm 34 \text{ kg m}^{-2}$ (JJA). However, in the ablation area, long-term cloud radiative warming is caused due to an increased absorption of SW radiation, rather than the expected increase of net LW radiation; see Figures 3b and 3c. This can be explained by the accompanying decrease in albedo (Figure 3d) on the long-term time scale, enhancing SW radiation absorption. This subsequently increases the surface melt rates and results in a cloud-reduced SMB. Contrarily, the small long-term cloud cooling effect in the accumulation area has a small cloud-enhanced SMB impact $0.1 \pm 0.1 \text{ kg m}^{-2}$ (MAM) and $0.5 \pm 0.9 \text{ kg m}^{-2}$ (JJA).

A specifically outstanding feature is the small coastal strip in the southwest of the GrIS. In this area, short-term cloud radiative warming occurs in spring (Figure 1b) but the impact is a short-term cloud-enhanced SMB, as seen in Figure 2b. This is further discussed in section 3.3.

Though the impact of summer cloud radiative cooling over the ablation area is stronger per unit area than the warming effects in the accumulation area, the latter occurs year-round through its impact on

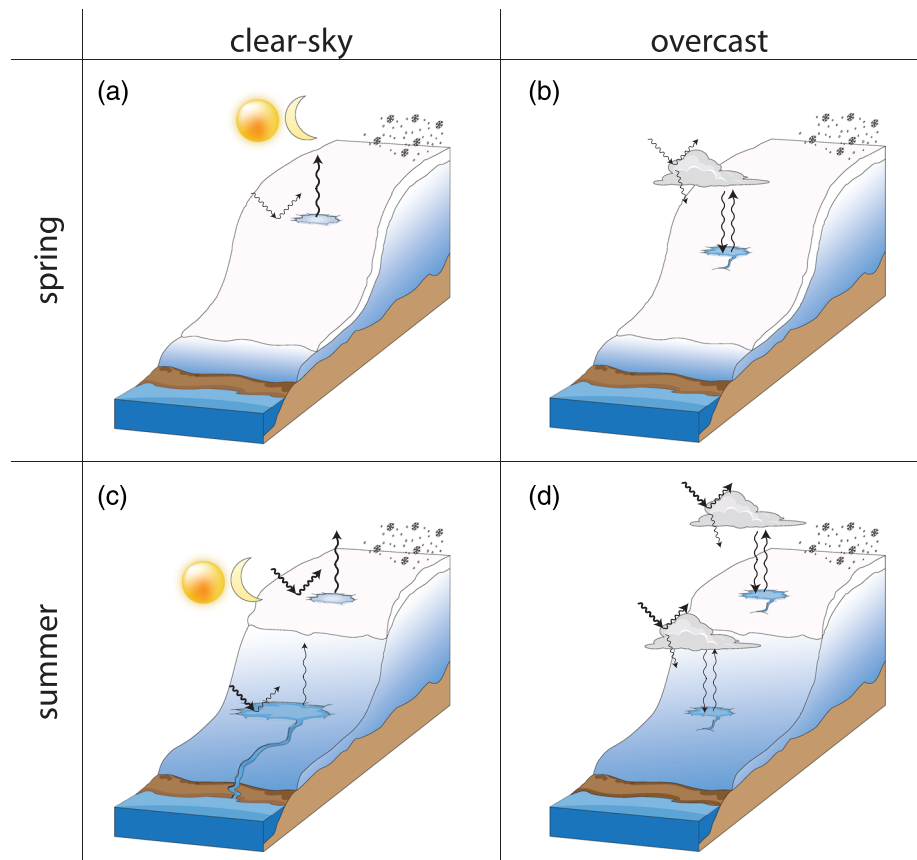


Figure 4. Schematic representation of typical spring (a, b) and typical summer (c, d) surface conditions and impact of cloud radiative forcing. Visualized for a typical clear-sky (a, c) or overcast (b, d) scenario. For summer, a clear distinction is made between the ablation area (dark) and accumulation area (white). Precipitation is the same for both scenarios.

sublimation, as well as over a roughly tenfold larger area. As a result, the annual area-integrated impact is total cloud-reduced SMB of $-157 \pm 3.8 \text{ Gt yr}^{-1}$ while the total cloud-enhanced SMB is $121 \pm 2.2 \text{ Gt yr}^{-1}$, resulting in a net impact of -36 Gt yr^{-1} on the SMB—a relative mass loss due to clouds.

Noting that the ablation area is expected to expand in the coming decades, this balance is expected to shift more to cloud-reduced mass loss impacts.

3.3. Underlying Processes

We have discussed how the short-term cooling effect of clouds leads to an albedo increase, while the long-term cloud warming results in an albedo decrease (Figure 3, section 3.2). Apart from the CRE on the albedo-SW feedback, the initial albedo as well as the amount of SW radiation determine the strength of these feedbacks. The balance of these parameters is most delicate during spring. As mentioned before, at the coast of west GrIS the cloud radiative warming effects results in a cloud-enhanced SMB (relative mass increase). This paradox can be explained by the sensitivity of the surface to the initial albedo and the albedo melt feedback, in combination with the long-term impact of clouds on the albedo. The impact of the short-term spring cloud radiative warming on the SMB depends on the strength of the CRE (which is weak) and the conditions of the surface: This area is relatively dark (low albedo, supporting information Figure S6), resulting in a strong albedo melt feedback which favors SW cooling effects over LW warming effects and results in net cloud-enhanced SMB. Supporting information Figure S7 shows the relation between the short-term impact on the SMB and the initial albedo. In spring, a low albedo can result in either cloud-enhanced or cloud-reduced SMB, depending on the CRE strength. During the summer period, cloud-reduced SMB (relative mass loss) solely occurs for high initial albedo values, indicating that at darker areas the albedo melt feedback always dominates.

This balance between the surface conditions, the strength of the short-term CRE and its impact on the SMB emphasize the important role of the long-term CRE in tipping the scale: In areas where long-term cloud warming decreases the albedo, the onset of the summer melt period is advanced.

The abovementioned variations of the temporal and spatial impacts of cloud radiative forcing are schematically represented in Figure 4. During typical spring conditions, a net cloud radiative warming is found for both short-term and long-term components, and the initial albedo is typically high. This implies that, if melt occurs, it will refreeze in clear-sky conditions (Figure 4a) but not in overcast conditions (Figure 4b): clouds increase run-off—a cloud-reduced SMB. An important condition for this process to occur is that the initial albedo is high, or little SW radiation is received by the surface. Areas where the initial albedo is lower will more quickly transition to the “typical summer” scheme, outlined in Figure 4c.

In typical summer conditions, the ablation area has experienced melt already, and therefore, the albedo is lower than during spring. As a consequence, a lot of SW radiation is absorbed during a clear-sky day (Figure 4c), further enhancing melt. In this case, overcast conditions reduce the amount of available energy significantly: SW reduction is stronger than LW enhancement. The net result is cloud-enhanced SMB—a relative mass increase. Meanwhile, in the accumulation area (Figure 4d), the effects of a cloudy or clear-sky day are similar to the typical spring conditions.

The long-term effect of clouds is important to take into account in this: The long-term cloud warming effect in spring decreases the albedo, resulting in enhanced SW absorption for all succeeding conditions. This long-term effect can determine the timing of the onset of the “typical summer” conditions described in the figure.

4. Discussion and Conclusion

Our results demonstrate the complex role cloud radiation has on the GrIS SMB, showing strong temporal variations and spatial contrasts. This indicates that for any study, the choice of spatiotemporal coverage and resolution influences what type of cloud effects will be found: cloud radiative cooling in the summer ablation area, or year-round cloud radiative warming over the complete GrIS. With the improved understanding of the underlying processes, we can bring multiple studies together and diminish the conflicting views that previously existed. In agreement with Wang et al. (2018); Ruan et al. (2019); Hofer et al. (2017), we show that clouds limit the albedo-melt feedback and decelerate surface melt. We add that this is only the case for the summer ablation area or dark albedo areas; not for other seasons, the accumulation area or high albedo areas. The spatial contrasts are similar to Wang et al. (2019). However, we also link cloud warming effects to a relative loss of mass, in agreement to Van Tricht et al. (2016), and show that this occurs year-round through sublimation impacts. Annually, the warming effect dominates the cooling effect, yielding net cloud-reduced SMB; a relative mass loss. We expect this balance to shift more to a net cloud-enhanced SMB impact due to expected growth of the size of the ablation area, which will increase cloud cooling effects. Besides this, we must note that in reality this balance is likely already shifted a bit more to the cloud cooling effects/cloud-enhanced SMB due to two factors. First, by excluding changes in precipitation in our scenarios, snowfall occurs in clear-sky conditions. As a result, the cloud-enhanced SMB is likely larger in reality due to absence of snowfall. Second, as SNOWPACK underestimates the ablation rate, cloud cooling effects and thus the cloud-enhanced SMB are underestimated as well.

Furthermore, we took the average of two different short-term components for the benefit of clear figures and numbers. However, the different response of the GrIS to the same all-sky/clear-sky scenario on different surface conditions could provide further understanding of the processes that determine the impact of the CRE.

We brought attention to the importance of the initial surface conditions, and in that respect, the significance of the long-term cloud radiative warming effect that changes these conditions and increases the potential for summer melt. This means that for future studies, the need for an accurate albedo parameterization is paramount, to capture the right albedo melt feedback.

Lastly, we conclude that to better understand the future role of cloud radiation on the GrIS, their spatial and temporal patterns must be known. A decrease in cloud cover will increase surface melt in the ablation area, or vice versa. As the cloud radiative cooling effect, and subsequent cloud-enhanced SMB, is a stronger

impact on the SMB per unit area than the cloud radiative warming effects, an expansion of the ablation zone could cause a strong shifts in the SMB due to cloud presence/absence.

Data Availability Statement

RACMO2.3p2 model data are available at this site (<https://www.projects.science.uu.nl/iceclimate/models/racmo.php>). The SNOWPACK model is open source, available via the WSL Institute for Snow and Avalanche Research SLF (<https://models.slf.ch>). The simulation results are available at the 4TU research data repository (<https://data.4tu.nl/>) with uuid:5126dbc6-f97a-4b90-be10-ea9ebe1d35c8.

Acknowledgments

RACMO2.3p2 model data have been provided by the Institute for Marine and Atmospheric Research Utrecht (IMAU), the Netherlands.

References

- Bintanja, R., & Van Den Broeke, M. R. (1996). The influence of clouds on the radiation budget of ice and snow surfaces in Antarctica and Greenland summer. *International Journal of Climatology*, *16*(11), 1281–1296. [https://doi.org/10.1002/\(SICI\)1097-0088\(199611\)16:11<1281::AID-JOC83>3.0.CO;2-A](https://doi.org/10.1002/(SICI)1097-0088(199611)16:11<1281::AID-JOC83>3.0.CO;2-A)
- Box, J. E., Fettweis, X., Stroeve, J. C., Tedesco, M., Hall, D. K., & Steffen, K. (2012). Greenland ice sheet albedo feedback: Thermodynamics and atmospheric drivers. *The Cryosphere*, *6*(4), 821–839. <https://doi.org/10.5194/tc-6-821-2012>
- Curry, J. A., Rossow, W. B., Randall, D., & Schramm, J. L. (1996). Overview of Arctic cloud and radiation characteristics. *Journal of Climate*, *9*, 1731–1764. [https://doi.org/10.1175/1520-0442\(1996\)009<1731%3A0OACAR>2.0.CO;2](https://doi.org/10.1175/1520-0442(1996)009<1731%3A0OACAR>2.0.CO;2)
- Fettweis, X., Franco, B., Tedesco, M., van Angelen, J. H., Lenaerts, J. T. M., van den Broeke, M. R., & Galle, H. (2013). Estimating Greenland ice sheet surface mass balance contribution to future sea level rise using the regional atmospheric climate model MAR. *The Cryosphere*, *7*, 469–489. <https://doi.org/10.5194/tc-7-469-2013>
- Fettweis, X., Hanna, E., Lang, C., Belleflamme, A., Erpicum, M., & Galle, H. (2013). Brief communication important role of the mid-tropospheric atmospheric circulation in the recent surface melt increase over the Greenland ice sheet. *The Cryosphere*, *7*, 241–248. <https://doi.org/10.5194/tc-7-241-2013>
- Gardner, A. S., & Sharp, M. J. (2010). A review of snow and ice albedo and the development of a new physically based broadband albedo parameterization. *Journal of Geophysical Research*, *115*, F01009. <https://doi.org/10.1029/2009JF001444>
- Hofer, S., Tedstone, A. J., Fettweis, X., & Bamber, J. L. (2017). Decreasing cloud cover drives the recent mass loss on the Greenland ice sheet. *Science Advances*, *3*, e1700584.
- Lehning, M., Bartelt, P., Brown, B., Fierz, C., & Satyawali, P. (2002). A physical SNOWPACK model for the Swiss avalanche warning: Part II. Snow microstructure. *Cold Regions Science and Technology*, *35*, 147–167.
- Ruan, R., Chen, X., Zhao, J., Perrie, W., Mottram, R., Zhang, M., et al. (2019). Decelerated Greenland ice sheet melt driven by positive summer north Atlantic oscillation. *Journal of Geophysical Research: Atmospheres*, *124*, 7633–7646. <https://doi.org/10.1029/2019JD030689>
- van Angelen, J. H. (2012). Sensitivity of Greenland ice sheet surface mass balance to surface albedo parameterization: A study with a regional climate model. *The Cryosphere*, *6*, 1175–1186.
- Van Tricht, K., Lhermitte, S., Lenaerts, J. T. M., Gorodetskaya, I. V., L'Ecuyer, T. S., Noel, B., et al. (2016). Clouds enhance Greenland ice sheet meltwater runoff. *Nature Communications*, *7*, 10266. <https://doi.org/10.1038/ncomms10266>
- Van Wessem, J. M., van de Berg, W. J., Noël, B. P. Y., van Meijgaard, E., Amory, C., Birnbaum, G., et al. (2018). Modelling the climate and surface mass balance of polar ice sheets using RACMO2 – Part 2: Antarctica (1979–2016). *The Cryosphere*, *12*(4), 1479–1498. <https://doi.org/10.5194/tc-12-1479-2018>
- van den Broeke, M. R., Enderlin, E. M., Howat, I. M., Kuipers Munneke, P., Nol, B. P., Jan Van De Berg, W., et al. (2016). On the recent contribution of the Greenland ice sheet to sea level change. *The Cryosphere*, *10*, 1933–1946. <https://doi.org/10.5194/tc10-1933-2016>
- Wang, W., Zender, C. S., & van As, D. (2018). Temporal characteristics of cloud radiative effects on the Greenland ice sheet: Discoveries from multiyear automatic weather station measurements. *Journal of Geophysical Research: Atmospheres*, *123*, 11,348–11,361. <https://doi.org/10.1029/2018JD028540>
- Wang, W., Zender, C. S., van As, D., & Miller, N. B. (2019). Spatial distribution of melt season cloud radiative effects over Greenland: Evaluating satellite observations, reanalyses, and model simulations against in situ measurements. *Journal of Geophysical Research: Atmospheres*, *124*, 57–71. <https://doi.org/10.1029/2018JD028919>